ELSEVIER

Earth and Planetary Science Letters 197 (2002) 51–64

EPSL

www.elsevier.com/locate/epsl

The Santa Rosa Event: $^{40}Ar/^{39}Ar$ and paleomagnetic results from the Valles rhyolite near Jaramillo Creek, Jemez Mountains, New Mexico

Brad Singer [a,*], Laurie L. Brown [b]

[a] *Department of Geology and Geophysics, University of Wisconsin-Madison, 1215 West Dayton Street, Madison, WI 53076, USA*
[b] *Department of Geosciences, University of Massachussetts, Amherst, MA 01003, USA*

Received 20 August 2001; received in revised form 30 November 2001; accepted 4 December 2001

Abstract

The Jaramillo Event was originally defined by Doell and Dalrymple in 1966 on the basis of K–Ar ages from sanidine in the normally, transitionally and reversely magnetized rhyolite domes named Cerro del Abrigo, Cerro Santa Rosa I and Cerro Santa Rosa II, respectively, that erupted following collapse of the archetypal Valles Caldera, New Mexico. We have collected new paleomagnetic data from the three domes and new $^{40}Ar/^{39}Ar$ laser fusion and furnace incremental heating experiments on sanidine crystals from the Cerro Santa Rosa I rhyolite. Step-wise alternating field and thermal demagnetization techniques applied to 52 samples from seven sites indicate that the original paleomagnetic results of Doell and Dalrymple [Science 152 (1966) 1060–1061] are valid. Cerro del Abrigo is normally magnetized, whereas the Santa Rosa I dome is transitional with an inclination of −63° toward the east and the Santa Rosa II dome is of reversed polarity. Twenty-five laser fusion experiments on sanidine crystals from the the Cerro Santa Rosa I dome, together with the saddle-shaped spectrum obtained by incrementally heating the sanidine in a furnace reveal that this rhyolite contained a small but significant component of excess argon prior to eruption. Our preferred age of 936 ± 8 ka (± 2σ) for the Santa Rosa I rhyolite is based on the concordant laser fusion isochron and incremental heating plateau ages. This age is significantly older than was inferred on the basis of earlier laser fusion $^{40}Ar/^{39}Ar$ results that suggested a trapped component characterized by a $^{40}Ar/^{36}Ar$ ratio lower than the atmospheric value of 295.5. Our new age distinguishes the Santa Rosa I dome by 65 kyr from the termination of the Jaramillo normal subchron 1001 ± 10 ka and by 37 kyr from basaltic lavas at Haleakala and Tahiti, which record the Kamikatsura Event 899 ± 6 ka. Moreover, this determination is a factor of three more precise than the best previous estimate for a proposed geomagnetic event in this time period. The Cerro Santa Rosa I rhyolite dome, once intimately linked with the end of the Jaramillo Event and the acceptance of plate tectonic theory, now defines a highly resolved feature, the Santa Rosa Event, in a terrestrial geomagnetic reversal time scale that is consistent with the global record of magnetic field intensity from marine sediments.

Keywords: Ar-40/Ar-39; paleomagnetism; Jaramillo subchron; time scales; sanidine; rhyolites

* Corresponding author. Tel.: +1-608-265-8650; Fax: +1-608-262-0693.
E-mail addresses: bsinger@geology.wisc.edu (B. Singer), lbrown@geo.umass.edu (L.L. Brown).

0012-821X/02/$ – see front matter
PII: S0012-821X(01)00598-2

1. Introduction

In 1966, Doell and Dalrymple [1], on the basis of data from rhyolites of the Valles Caldera in northern New Mexico, identified and dated using the K–Ar method a normal polarity event within the reversed Matuyama chron. They named it the Jaramillo, after a creek that drains the Valles Caldera close to the rhyolite domes where the event was found. The importance of the Jaramillo Event to the new, yet controversial, geomagnetic polarity time scale, and hence to the entire development of the theory of plate tectonics, has been well established [2,3].

At the same time the future of K–Ar dating was foreshadowed when the power of its variant, the $^{40}Ar/^{39}Ar$ method, was revealed by Merrihue and Turner in 1966 [4]. The past 35 years have witnessed remarkable advances in the $^{40}Ar/^{39}Ar$ dating of Quaternary volcanic rocks using either a laser probe to degas sanidine phenocrysts, e.g. [3], or a resistance furnace to incrementally heat basalt groundmass, e.g. [5,6]. With analytical uncertainty of better than 1%, questions have evolved from: What are the ages of the major normal and reversed polarity chrons? and Do these agree with astronomically derived ages [5]? to: What are the precise ages of reversals, excursions, events and associated paleointensity changes that mark important changes in the geodynamo? and How many times did the geomagnetic field reverse, or attempt to reverse? [6–8].

Laser probe $^{40}Ar/^{39}Ar$ studies of Spell and McDougall [9], Spell and Harrison [10] and Izett and Obradovich [3] raised questions regarding the true age of the Jaramillo Event but neither precisely resolved its timing, nor addressed the possibility that a younger polarity event may be recorded in the Valles rhyolite domes. Moreover, modern demagnetization and rock magnetic methods [11,12] have not been applied to the Valles rhyolite to justify the original paleomagnetic data and determine whether other polarity events were recorded. We have collected new samples from the rhyolite domes of the Valles Caldera near Jaramillo Creek to further investigate the age and paleomagnetic signature of these rocks so critical to modern geology.

2. Geologic setting and previous work

The Jemez Mountains of north-central New Mexico comprise $\sim$2000 km^3 of late Miocene to Pleistocene volcanic deposits between the Rio Grande rift to the east and Colorado Plateau to the west (Fig. 1). Volcanism commenced 16.5 Ma and culminated with two catastrophic eruptions forming a 20 km diameter epicontinental caldera [13–16]. Following eruption of the lower Bandelier Tuff (Otowi member) at 1.637 ± 0.011 Ma ([3]; all uncertainties reported at the 2σ level and ages recalculated where necessary to intercalibration values below) that formed the Toledo Caldera, the upper Bandelier Tuff (Tshirege member) erupted at 1.241 ± 0.018 Ma and formed the Valles Caldera at about the same location. From the pioneering field and stratigraphic studies of Bailey, Smith, Doell and Dalrymple, [13,14,17] the Valles Caldera and its post-collapse rhyolites have become synonymous with caldera formation and evolution. The post-collapse rhyolites erupted along a ring fracture and form domes, dome complexes, flows, and pyroclastic rocks on the floor of the Valles Caldera (Fig. 1). We have re-investigated the paleomagnetism of three of the post-collapse domes from which Doell et al. [17] reported paleomagnetic and K–Ar results, including Cerro del Abrigo III, Cerro Santa Rosa I and Cerro Santa Rosa II (Fig. 1; Table 1). We have also acquired new $^{40}Ar/^{39}Ar$ data from sanidine of the Cerro Santa Rosa I rhyolite dome.

To date sanidine phenocrysts in these domes, Spell and Harrison [10] used an $^{40}Ar/^{39}Ar$ laser fusion technique to generate isochrons. Izett and Obradovich [3] used a similar approach to derive multiple total fusion ages that were pooled together to yield a mean age estimate for each dome. Although results of the two studies were generally in agreement, it is worth noting some of the problems. For example, the ages determined for the normally magnetized Cerro del Abrigo III dome of 1019 ± 19 ka [3] and 977 ± 19 ka [10] differ from one another by $>4\%$. The latter age is based on an isochron that combines 13 analyses of sanidine from all three Cerro del Abrigo domes (Fig. 1). Using the data of [10] we calculated the weighted mean age of seven of

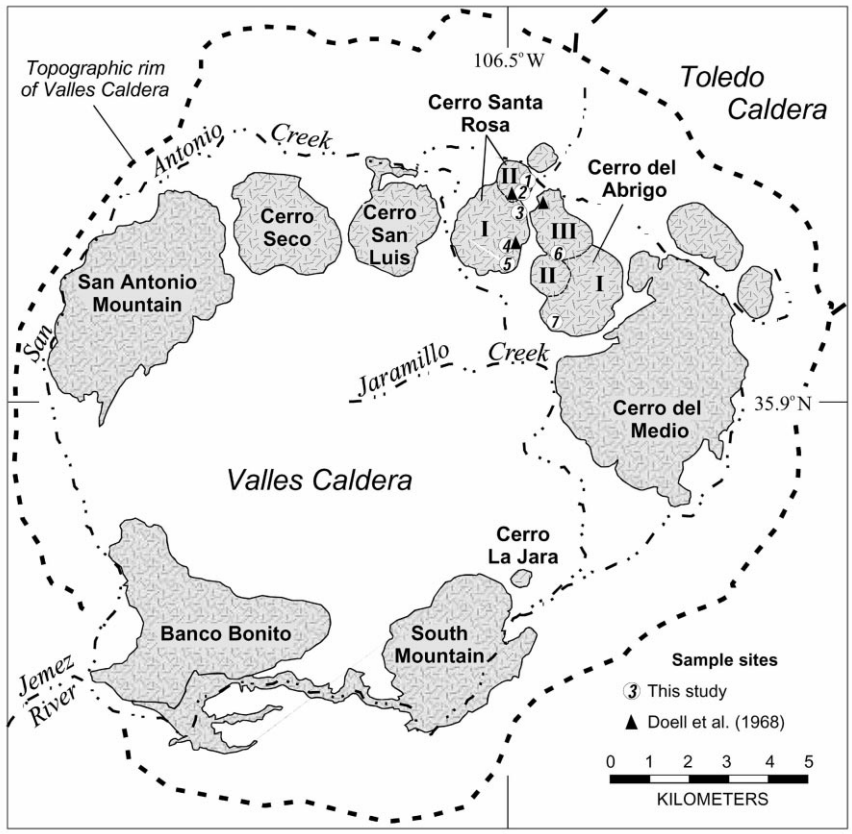

Fig. 1. Geologic map of Valles Caldera and post-collapse rhyolites. Adapted from Doell et al. [17] and Smith et al. [14].

these 13 analyses that were obtained exclusively from sanidine of the Cerro del Abrigo III dome, at 1000 ± 32 ka; this brings the age determinations of [3] and [10] into agreement and indicates that the Cerro del Abrigo III dome acquired its magnetization during the Jaramillo normal subchron which lasted from 1069 to 1001 ka [6]. Moreover, from the Santa Rosa I dome (Fig. 1; Table 1) Spell and Harrison [10] obtained a 919 ± 8 ka isochron from 16 of 19 total fusion measurements, but the trapped component defined by the $^{40}Ar/^{36}Ar$ intercept was 281.8 ± 9.4, significantly lower than the atmospheric value of 295.5, which is difficult to explain for terrestrial volcanic rocks [18]. From a split of the same sanidine separate analyzed by Doell et al. [17] from the Santa Rosa I rhyolite, Izett and Obradovich [3] obtained total fusion measurements from six multigrain aliquots that define a weighted mean age of 930 ± 17 ka. Concerned by the non-atmospheric trapped component found by Spell and Harrison [10], and the large uncertainty of Izett and Obradovich's [3] age determination, we undertook new $^{40}Ar/^{39}Ar$ laser fusion and furnace incremental heating experiments on sanidine from the Santa Rosa I dome.

3. Paleomagnetic and $^{40}Ar/^{39}Ar$ sampling and methods

Samples were collected from the steep sides of the three domes in 1994 using a gasoline powered drill. The number and location of sites established was limited by extensive unstable areas of loose blocks and slabs of rhyolite (Fig. 1). From three to 11 core samples were drilled in situ from each bedrock outcrop site and oriented using a sun

compass and clinometer. Natural remanent magnetization directions in all cores were measured using a 2 G cryogenic magnetometer at the University of Massachussetts. Demagnetization treatments used either a Schonstedt AF demagnetizer or an ASC thermal unit, and were done on all samples. Hysteresis measurements and susceptibility-temperature measurements were done at the Institute for Rock Magnetism at the University of Minnesota. All samples showed moderate NRM intensities averaging 0.71 A/m, and a progressive decrease in intensity during step-wise demagnetization.

Two drill cores from the coarsely sanidine and quartz porphyritic rhyolite at site VGR-3 on Cerro Santa Rosa I (Fig. 1) totalling 35 g were crushed, sieved, and the 250–500 μm fraction of sanidine was separated using magnetic susceptibility, heavy liquids and ultimately hand picking under a binocular microscope. To remove adhered glass, the purified sanidine was cleaned ultrasonically in cold 10% HF for 10 min and rinsed in deionized water. This procedure was similar to that of Izett and Obradovich [3] who used 24% HF, but differs from Spell and Harrison's [10] use of 5% HCl. The cleaned sanidine was loaded into pure Cu or Al foil packets and together with packets of neutron fluence monitor minerals placed into 5 mm i.d. quartz tubes that were evacuated and sealed prior to irradiation. Irradiations were done at the Oregon State University TRIGA reactor in the cadmium lined in core irradiation tube (CLICIT) for 60 min; samples received a fast neutron dose of $\sim 9\times10^{16}$ n/cm^2. On the basis of previous work [6], corrections for undesirable neutron-induced reactions on ^{40}K and ^{40}Ca are follows: $[^{40}Ar/^{39}Ar]_K = 0.00086$; $[^{36}Ar/^{37}Ar]_{Ca} = 0.000264$; $[^{39}Ar/^{37}Ar]_{Ca} = 0.000673$. All ages were calculated using decay constants of [19].

At the University of Wisconsin-Madison Rare Gas Geochronology Laboratory, crystals were loaded into wells on a copper planchette. Initial experiments involved degassing five crystals (<1 mg) of VGR-3 sanidine at once and measuring the isotopic composition of the gas. Subsequent experiments were undertaken on larger multigrain aliquots of 2–4 mg ($\sim$20 to 100 crystals) each. The crystals were heated to fusion in 60 s using a CO_2 laser and defocused beam that delivered 5–9 W to the samples. Following three additional minutes of clean up on a single SAES C-50 getter, the gas from each heating step was expanded into a Mass Analyser Products-215-50 spectrometer fitted with a Nier type ion source, the mass range 40–36 was scanned eight times in static mode using a Balzers SEV-17 electron multiplier, and its initial composition determined by regression analysis. System blanks were measured before every fourth sample and for ^{40}Ar were one to two orders of magnitude smaller than the samples ($\sim 10^{-17}$ mol), whereas for ^{36}Ar blanks typically comprised 10–90% of the signal ($\sim 10^{-19}$ mol), but were stable during analytical periods of several hours per session.

A 60 mg packet of VGR-3 sanidine was loaded into a stainless steel carousel over an automated double-vacuum resistance furnace and degassed at 500°C to remove adsorbed atmospheric argon. The incremental heating experiment consisted of 13 steps from 600 to 1550°C controlled via a tungsten–rhenium thermocouple, each involving 2 min of increase to the set-point temperature that was maintained for 10 min with the gas exposed to a SAES C50 getter operating at 450°C. Following five more minutes of clean-up with additional getters at 450 and 20°C, the purified gas was measured in the MAP 215-50 spectrometer as above. The 1100°C furnace blank measured prior to the experiment was about three times that of the laser blanks. During two different analytical periods more than 1 yr apart, mass discrimination was monitored using an on-line air pipet and was 1.0034 ± 0.0001 and 1.0025 ± 0.0001 per amu.

For each analysis the 2σ errors include estimates of the analytical precision on peak signals, the system blank, and spectrometer mass discrimination. Inverse-variance weighted mean (and plateau) ages were calculated according to [20]. The uncertainty in the neutron fluence parameter J was $<0.6\%$ (2σ) which was propagated into the final plateau, weighted mean, and isochron ages. Where the weighted mean or isochron calculations resulted in an MSWD (or sums/$(n-2)$) greater than unity, the uncertainty about the mean age was increased by multiplying by the

$\sqrt{\text{MSWD}}$. Isochrons were regressed using the method of York [21].

The $^{40}Ar/^{39}Ar$ method is a relative dating technique in which the age of a sample is calculated against mineral standards that have been previously dated. One packet containing 16 mg of VGR-3 sanidine was irradiated using Alder Creek rhyolite sanidine (ACs) as the neutron fluence monitor, whereas the two other packets containing 60 and 30 mg each were monitored using Taylor Creek rhyolite sanidine (TCs) as a standard and a packet of ACs for cross checking. The age of ACs has been determined at 1.194 Ma relative to 98.79 Ma for GA-1550 biotite and is intercalibrated to ages of 28.34 Ma for TCs and 28.02 Ma for Fish Canyon Tuff sanidine (FCs) [22]. We recognize that the age of the GA-1550 primary standard remains controversial [23–25]. Our decision to use the above values is based, in part, upon improved agreement between $^{40}Ar/^{39}Ar$ and astronomical ages for the last several reversals of the geomagnetic field [26]. The neutron fluence parameter J was determined by pooling 5–7 laser fusion measurements of crystals from monitor packets adjacent to the VGR-3 sanidine samples. Using 28.34 Ma for the TCs monitors, five measurements of ACs standard grains gave a weighted mean of 1.192 ± 0.012 Ma that is identical with the 1.194 ± 0.014 Ma calibration of this standard [22].

4. Results

4.1. Paleomagnetism

Natural remanent magnetization and demagnetization behavior were measured on a total of 52 independent samples from seven sites on the three domes (Fig. 1, Table 1). Typical step-wise demagnetization patterns from alternating field (AF) and thermal experiments (Fig. 2) show that in most samples AF fields of 10–20 mT were sufficient to remove a weak viscous component and successive fields up to 80 mT produced linear principal component vectors that trend toward the origin (Fig. 2A,C,D). Thermal demagnetization to 300°C removed the secondary component and from 300 to 575°C well-defined vectors trending toward the origin were unblocked that are

Table 1
Paleomagnetic directions from selected Valles Caldera post-collapse rhyolite domes, Jemez Mountains, New Mexico

Site	*N*/*No.*	INC	DEC	*k*	α95	VGP latitude/longitude
Cerro Santa Rosa II:						
VGR-1	8/8	−50.7	209.8	184	3.6	−65/165
VGR-2	8/9	−53.4	192.8	222	3.3	−79/171
S40[a]	7/8	−55.1	194.8	129	5.3	−78/161
Mean	3/3	−53.3	199.4	119	9.3	
Cerro Santa Rosa I:						
VGR-3	8/9	−55.8	103.6	67	6.1	−30/9
VGR-4	9/9	−66.5	292.3	13	12.8	−14/112
VGR-5	6/8	−65.7	106.7	129	5.0	−36/21
S39[a]	7/8	−67.4	99.4	305	3.5	−32/25
Mean	3/4	−63.0	103.4	105	9.8	
Cerro del Abrigo:						
VGR-6	2/3	50.6	18.9	159	14.1	74/353
VGR-7	11/11	49.6	13.6	114	4.0	77/6
S37[a]	7/7	50.8	23.7	62	7.7	70/349
Mean	3/3	50.4	18.7	404	5.0	

N/*No.*, number of samples used in calculations versus number collected; INC, DEC, inclination and declination in degrees; *k*, precision parameter of Fisher [41]; α95, cone of 95% confidence about mean direction; VGP, corresponding virtual geomagnetic pole, in degrees latitude/longitude.
[a] Sites from Doell et al. [17].

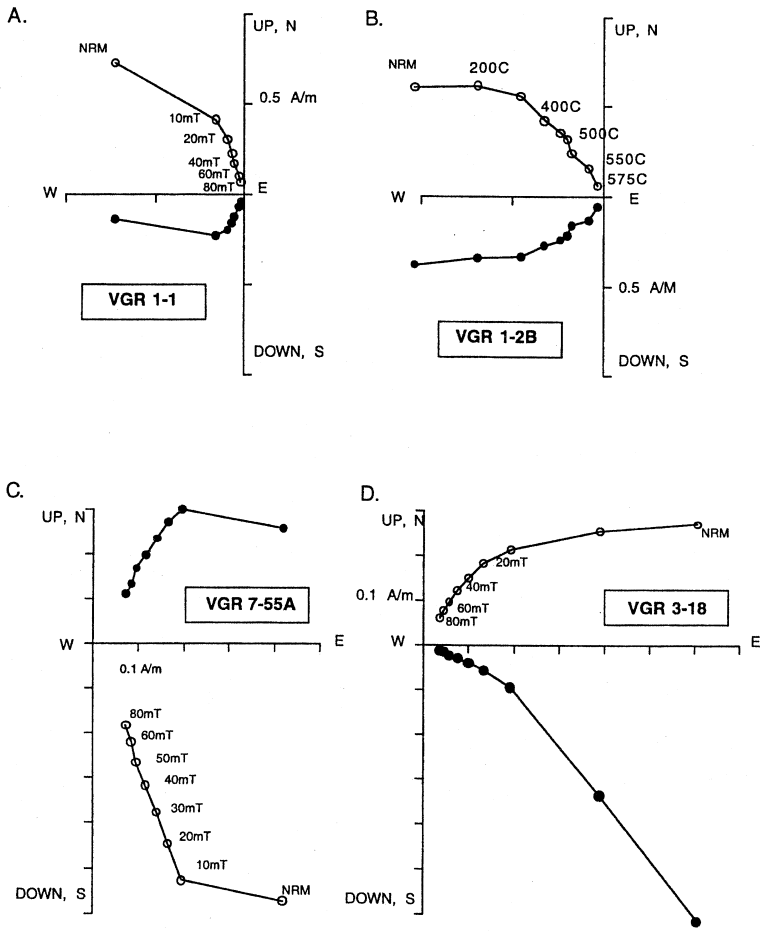

Fig. 2. Orthogonal projections of representative samples during AF and thermal demagnetization. Horizontal component = filled symbols; vertical = open symbols. (A) and (B) compare AF and thermal demagnetization treatment of samples from site 1 on Santa Rosa II dome (Fig. 1). (C) and (D) show AF demagnetization of samples from site 7 on Cerro del Abrigo and site 3 on Santa Rosa I domes (Fig. 1).

indistinguishable from those obtained from other samples at the same site using AF treatment (Fig. 2A,B).

Hysteresis measurements on one sample from each site are typical of fine-grained magnetite, with narrow S-shaped curves and saturation between 0.1 and 0.3 T. The ratio of saturation remanence to saturation magnetization (M_r/M_s) ranges from 0.094 to 0.309, and the comparison of coercivity of remanence to coercive force (H_{cr}/H_c) ranges from 1.7 to 3.6. Placed in a Day plot (Fig. 3), all data lie in the pseudo-single domain (PSD) field, trending from the multidomain field towards the single domain field. The highest coercivity ratio is from site VGR-4, one of the transitional sites from Cerro Santa Rosa I. The hysteresis data show that the principal magnetic carrier in the Valles Grande rhyolites is fine-grained magnetite.

Paleomagnetic directions and virtual geomagnetic poles (VGPs) for the seven sites were compared to those of Doell et al. [17] obtained from a single site on each of the three domes (Fig. 1; Table 1). The new paleomagnetic directions obtained from all sites except VGR-4 are nearly identical to previous results [17] or, in the case

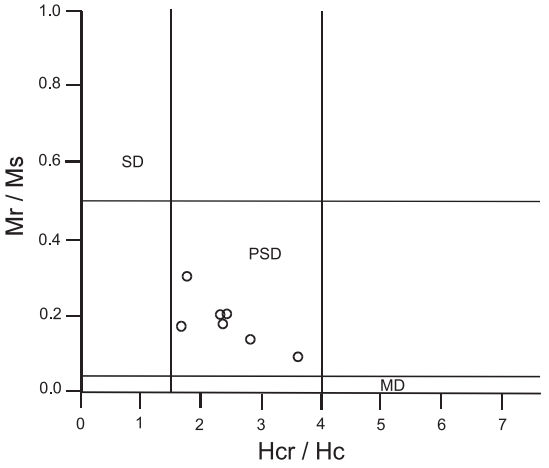

Fig. 3. Day plot [40] of hysteresis properties of one sample from each of the paleomagnetic sites. SD = single domain, PSD = pseudo-single domain, MD = multidomain. Horizontal axis is the ratio of coercivity of remanence to coercive force and vertical axis is the ratio of saturation remanence to saturation magnetization.

of VGR-1, not overlapping with but close to the other sites from that dome. Site VGR-4, from Cerro Santa Rosa I, is markedly different from the other sites on that dome, having a similar steep negative inclination, but a declination about 180° apart. The mean results (Table 1) indicate: (1) a steep positive inclination and north declination are preserved in Cerro del Abrigo rhyolite, (2) a steeply inclined but east direction was recorded by three of the four sites at Cerro Santa Rosa I, and (3) steep negative inclinations and a south declination characterize Cerro Santa Rosa II (Fig. 4).

4.2. Geochronology

Twenty-five $^{40}Ar/^{39}Ar$ laser fusion measurements of VGR-3 sanidine (Table 2) yielded a Gaussian distribution of apparent ages ranging from 903 ± 46 to 989 ± 39 ka with a probability maximum corresponding to the weighted mean of 947.5 ± 7.5 ka at an acceptably low MSWD of 1.56 (Fig. 5A). There are no clear-cut outliers, however, the analysis comprising by far the least radiogenic argon (46% $^{40}Ar^*$) is the only one with an apparent age, 979.7 ± 21.7 ka, that is distinguishable from the weighted mean on the basis of the 2σ uncertainties (Fig. 5A). Eliminating this analysis yields a weighted mean apparent age of 946.0 ± 7.0 ka with an MSWD of 1.20. Regressing all 25 analyses defines an isochron of 936.4 ± 7.9 ka with sums/$(n-2)$ of 1.10 that indicates a nonradiogenic trapped component with a $^{40}Ar/^{36}Ar_i$ of 307.3 ± 5.1 which is slightly, but significantly, higher than the atmospheric value of 295.5 (Fig. 5B). Omitting the least radiogenic analysis gave an isochron of 935.8 ± 8.4 ka with sums/$(n-2)$ of 1.14 and a $^{40}Ar/^{36}Ar_i$ ratio of 309.0 ± 8.0, therefore this analysis has virtually no influence on the results.

Apparent ages ranging from 934 ± 6 to 1198 ± 303 ka were generated during the incremental heating experiment producing a spectrum that is markedly saddle-shaped, with ages of both the initial and final gas increments higher than those of the eight steps comprising 93% of the gas released that define the plateau age of 936.9 ± 5.7 ka. The isochron defined by the eight plateau steps, 935.6 ± 8.0 ka, is indistinguishable from the plateau age with a poorly defined $^{40}Ar/^{36}Ar_i$ for the trapped component of 302.9 ± 41.9 that is broadly consistent with the atmospheric value. Regressing the five non-plateau steps defines an isochron of 950.0 ± 21.0 ka with a sums/

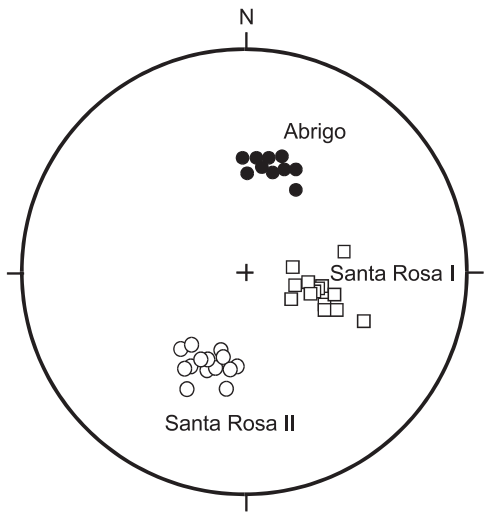

Fig. 4. Equal area projection of inclination and declination for individual sample data. Abrigo (site 7; $n = 11$ samples), Santa Rosa I (sites 3 and 5; $n = 14$), and Santa Rosa II (sites 1 and 2, $n = 16$).

Table 2
Total fusion and incremental heating $^{40}Ar/^{39}Ar$ data from sanidine of the Santa Rosa I rhyolite dome

Analysis number	Weight (mg)	$^{40}Ar/^{39}Ar$	$^{37}Ar/^{39}Ar$[a]	$^{36}Ar/^{39}Ar$	$^{40}Ar^*$ (10^{-15} mol)	^{39}Ar (% of total)	$^{40}Ar^*$ (%)	$^{40}Ar^*/^{39}Ar_K$	Apparent age[b] (ka ± 2σ)
Laser fusions		$J = 0.000266$		mass disc. = 1.0025 per amu			monitored with ACs (1.194 Ma)		
AA0117	< 1	2.16577	0.01055	0.000075	4.22		98.9	2.14356	954.9 ± 31.6
AA0118	< 1	2.17243	0.01138	0.000153	3.98		97.9	2.12720	947.6 ± 43.7
AA0132	< 1	2.30066	0.01218	0.000797	6.17		89.7	2.06516	920.0 ± 33.4
AA0133	< 1	2.22642	0.01181	0.000591	4.88		92.1	2.05165	914.0 ± 66.7
AA0134	< 1	2.20548	0.01154	0.000279	6.90		96.2	2.12299	945.8 ± 28.1
AA0154	< 1	2.21208	0.01100	0.000547	5.44		92.6	2.05027	913.4 ± 34.6
AA0155	< 1	2.20585	0.01202	0.000379	5.12		94.9	2.09377	932.8 ± 35.4
AA0156	< 1	2.20774	0.01076	0.000161	4.38		97.8	2.16007	962.3 ± 47.3
AA0158	< 1	2.30153	0.01093	0.000708	7.51		90.9	2.09213	932.0 ± 27.8
AA0159	< 1	2.18364	0.01081	0.000138	6.96		98.1	2.14286	954.6 ± 28.6
AA0160	< 1	2.20685	0.01148	0.000272	7.08		96.3	2.12638	947.3 ± 27.1
AA0161	< 1	2.22421	0.01124	0.000671	5.04		91.0	2.02578	902.5 ± 46.0
AA0163	< 1	2.23663	0.01167	0.000441	7.02		94.1	2.10615	938.3 ± 39.5
AA0164	< 1	2.34553	0.01114	0.000424	8.49		94.6	2.22028	989.1 ± 39.4
AA0166	< 1	2.25993	0.01182	0.000709	7.16		90.7	2.05044	913.5 ± 39.9
		$J = 0.000247$		mass disc. = 1.0034 per amu			monitored with TCs (28.34 Ma)		
AA6241	2	2.24341	0.01641	0.000437	11.86		94.2	2.11431	941.9 ± 14.0
AA6242	2	2.56337	0.01108	0.001475	14.52		83.0	2.12756	947.8 ± 13.7
AA6243	2	2.26362	0.01405	0.000481	10.90		93.7	2.12135	945.0 ± 14.4
AA6244	2	2.21274	0.01193	0.000325	14.27		95.6	2.11684	943.0 ± 12.7
AA6246	2	2.44600	0.01145	0.001121	10.16		86.4	2.11466	942.1 ± 26.9
AA6247	3	4.79102	0.01008	0.008771	20.72		45.9	2.19921	979.7 ± 21.7
AA6248	2	2.89470	0.01429	0.002566	12.41		73.8	2.13659	951.8 ± 17.6
AA6250	2	3.63163	0.01905	0.004911	11.62		60.0	2.18047	971.4 ± 22.0
AA6251	4	3.46703	0.01080	0.004486	16.31		61.7	2.14137	954.0 ± 19.5
AA6253	5	2.31532	0.01236	0.000625	21.20		92.0	2.13064	949.2 ± 9.6
								weighted mean $n = 25$	947.5 ± 7.5
								isochron $n = 25$	936.4 ± 7.9

Analysis number	Temp. (°C)	$^{40}Ar/^{39}Ar$	$^{37}Ar/^{39}Ar$[a]	$^{36}Ar/^{39}Ar$	$^{40}Ar^*$ (10^{-15} mol)	^{39}Ar (% of total)	$^{40}Ar^*$ (%)	$^{40}Ar^*/^{39}Ar_K$	Apparent age[b] (ka ± 2σ)
Incremental-heating		$J = 0.000243$	60 mg	mass disc. = 1.0034 per amu			monitored with TCs (28.34 Ma)		
AA6189	850°C	6.43927	0.00964	0.012540	0.18	0.15	42.45	2.73368	1198.0 ± 303.0
AA6190	950°C	2.85699	0.02868	0.002044	0.49	0.95	78.83	2.25289	987.4 ± 51.2
AA6191	1025°C	2.66228	0.03315	0.001570	0.82	1.70	82.55	2.19842	963.5 ± 31.7
AA6192	1100°C	2.29647	0.01998	0.000541	1.87	4.48	93.00	2.13662	936.4 ± 12.3
AA6193	1150°C	2.22219	0.01833	0.000251	2.14	5.30	96.62	2.14798	941.4 ± 9.8
AA6194	1225°C	2.21181	0.01656	0.000270	4.20	10.47	96.35	2.13190	934.4 ± 6.3
AA6195	1275°C	2.31603	0.01548	0.000608	5.14	12.23	92.21	2.13651	936.4 ± 6.6
AA6196	1325°C	2.19980	0.01388	0.000225	6.22	15.57	96.94	2.13334	935.0 ± 4.9
AA6197	1350°C	2.22791	0.01381	0.000269	3.57	8.83	96.39	2.14835	941.6 ± 8.4
AA6198	1400°C	2.21061	0.01624	0.000248	10.83	26.97	96.65	2.13740	936.8 ± 4.6
AA6199	1425°C	2.26317	0.01535	0.000390	3.71	9.02	94.87	2.14779	941.3 ± 8.7
AA6200	1475°C	2.81327	0.01815	0.002144	1.34	2.61	77.45	2.17960	955.3 ± 19.3
AA6201	1550°C	5.71203	0.01950	0.011585	1.78	1.72	40.06	2.28857	1003.0 ± 43.6
								plateau 1100–1425°C	936.9 ± 5.7
								isochron $n = 8$	935.6 ± 8.0

[a] Corrected for ^{37}Ar and ^{39}Ar decay, half-lives of 35.1 days and 269 years, respectively.
[b] Ages calculated relative to 1.194 Ma ACs or 28.34 Ma TCs [22]; using decay constants of [19]; uncertainties reported at 2σ.

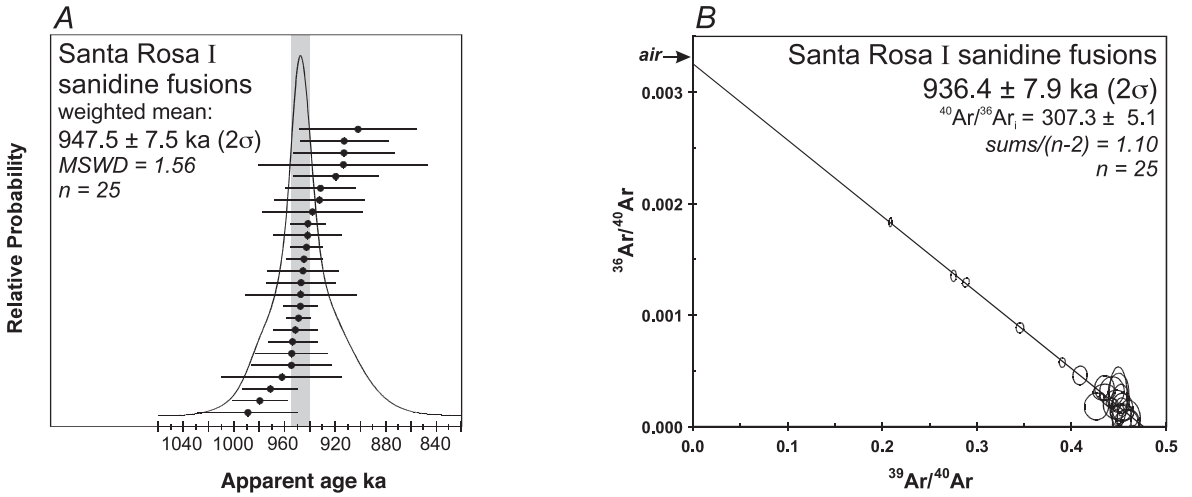

Fig. 5. (A) Cumulative probability diagram of apparent ages from 25 laser fusion analyses of sanidine from site VGR-3 on Cerro Santa Rosa I rhyolite dome. Vertical gray band defines weighted mean age of 947.5 ± 7.5 ka (± 2σ). (B) Isotope correlation diagram for the same 25 analyses shown in (A). The isochron defines a non-atmospheric intercept on the $^{36}Ar/^{40}Ar$ axis.

($n-2$) of 0.82 and $^{40}Ar/^{36}Ar_i$ of 307.0 ± 11.0, just higher than the atmospheric ratio.

The non-atmospheric y-axis intercept of the total fusion isochron (Fig. 5B) and the saddle-shaped age spectrum (Fig. 6A) indicate that some sanidine crystals entrapped gas that contained a small but distinguishable fraction of excess argon prior to eruption and setting of the K–Ar radioisotopic clock. The weighted mean apparent age from the laser fusion experiments of 947.5 ± 7.5 ka assumed that the trapped component was atmospheric in composition, hence this approach overestimates the time since eruption. The isochron (Fig. 5B) makes no assumption re-

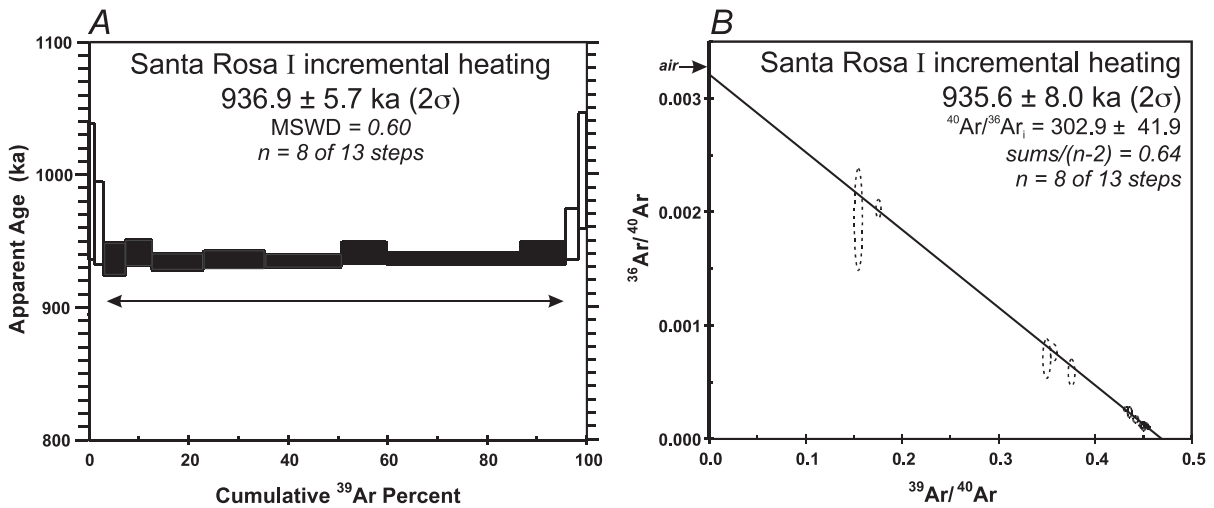

Fig. 6. (A) Age spectrum diagram derived from incremental heating of 60 mg of sanidine from site 3 on Cerro Santa Rosa I dome. Note the saddle-shaped spectrum with increments defining the plateau age filled. (B) Isotope correlation diagram from the incremental heating experiment in (A). Plateau data are small solid outlined points, non-plateau points are dashed.

garding the trapped component, thus we accept its age as the best estimate of time elapsed since eruption of the Santa Rosa I dome.

5. Discussion

5.1. Paleomagnetism

Despite obtaining paleomagnetic information using modern demagnetization procedures from over twice as many samples and sites of the three rhyolite domes, our results are entirely consistent with those of Doell et al. [17]. We confirm that Cerro del Abrigo, with consistent steep positive inclinations and north declinations, is normally magnetized, Cerro Santa Rosa I, with steep negative inclinations and either east or west declinations, is transitionally magnetized, and Cerro Santa Rosa II is reversely magnetized, marked by steep negative inclinations and south declinations. The presence of two statistically distinct, but transitional, directions from Cerro Santa Rosa I is consistent with a rapidly changing field during a magnetic field reversal during emplacement of the dome.

5.2. Excess argon in the Santa Rosa I rhyolitic magma

Recent experiments [27] on melt inclusions within quartz phenocrysts from the lower and upper Bandelier tuffs that erupted $\sim$700 and $\sim$300 kyr prior to the Santa Rosa I rhyolite indicate that the Bandelier rhyolite magma contained excess argon in quantities that could affect sanidine ages. In fact, Spell and Harrison [10] found that a small, yet detectable, level of excess argon was present in sanidine from the 803 ± 6 ka reversely magnetized Cerro San Luis dome that is adjacent to Cerro Santa Rosa I (Fig. 1). On the basis of Sr and Nd isotope and trace element differences, the Bandelier tuff magma is interpreted to have been produced through basalt-induced melting of hybridized Precambrian deep crustal rocks. Some of the post-caldera Valles rhyolites, including the Cerro San Luis and Santa Rosa I domes, tapped successive silicic magma reservoirs produced by later, much smaller, deep crustal melts that evolved independently from one another through crystallization and wall rock assimilation in shallow upper crustal reservoirs [28]. Thus, although the discovery of excess argon is not a complete surprise, its source in the San Luis and Santa Rosa I rhyolitic magmas may not have been identical to that in the preceding, larger Bandelier magma reservoir. Our results extend the conclusions of [27] demonstrating that an approach combining incremental heating and total fusion-isochron data are required to avoid spuriously old $^{40}Ar/^{39}Ar$ dates from sanidine not only in rapidly erupted and poorly outgassed rhyolitic ash flows, but in some slowly erupted and more thoroughly outgassed rhyolitic lava flows and domes as well. Indeed, the incremental heating experiment (Fig. 6A) effectively separates the excess argon from the dominant radiogenic component, hence the plateau (and the isochron defined by its steps) confirms an age for the transitionally magnetized Santa Rosa I rhyolite dome of 936 ± 8 ka. The difference between the weighted mean apparent age of 948 ka (Fig. 5A) and the isochron of 936 ka (Figs. 5B and 6B) implies that $>1\%$ of the ^{40}Ar in the sanidine crystals derives from excess argon present in the Santa Rosa I magma at the time of its eruption and growth of the dome.

5.3. Age of the Santa Rosa I dome

Our preferred age of 936 ± 8 ka for the Santa Rosa I dome does not differ from the Doell et al. [17] K–Ar age of 922 ± 56 ka, provided the latter is calculated using modern decay constants [19], reported with 2σ uncertainty, and increased 1.5% to reflect the difference in ages of standards used in the USGS laboratory [23,24] and the 28.34 Ma value that we have adopted for the TCs standard [22]. Nor does our isochron differ from the apparent age of 930 ± 17 ka obtained by Izett and Obradovich [3], but its precision is improved. At the 95% confidence level, our preferred age is, however, significantly older than the 919 ± 8 ka isochron age reported by Spell and Harrison [10].

Subtle problems with the analyses or cleaning of the sanidine separate may explain this discrep-

ancy. The isochron calculated by Spell and Harrison [10] for 16 of 19 laser fusion analyses has an $^{40}Ar/^{36}Ar_i$ value of 281.8 ± 9.4. Including all 19 analyses in their regression [10] yielded a $^{40}Ar/^{36}Ar_i$ value of 277.1 ± 14.2. Values of $^{40}Ar/^{36}Ar_i$ less than the atmospheric ratio of 295.5 are not produced on Earth by well understood radiogenic, cosmogenic, or contamination processes, hence the values obtained by [10] are curious and require an unusual and perhaps non-geological explanation. One possibility is that the HCl cleaning procedure [10] was inadequate to remove minor quantities of variably hydrated or altered K-rich silicic glass adhered to the sanidine crystals following crushing, sieving and heavy liquid separations. The presence of glass could pose several potentially problematic effects, for example: (1) altered glass may have lost some radiogenic argon [29], (2) hydrated glass may actually have lost K rather than radiogenic argon [30], (3) altered or hydrated glass may be susceptible to recoil of ^{39}Ar during neutron bombardment of the sample [31], and (4) hydration or alteration of glass may selectively fractionate ^{36}Ar from ^{40}Ar, thereby lowering its $^{40}Ar/^{36}Ar$ ratio [32].

In an isochron diagram (e.g. Fig. 5B), loss of K, translation of ^{39}Ar atoms via recoil out of the glass and into the sanidine lattice, or fractionation of ^{36}Ar could displace $^{39}Ar/^{40}Ar$ values to the right of the isochron or $^{36}Ar/^{40}Ar$ ratios above it. Such dispersion could bias the $^{40}Ar/^{36}Ar_i$ value of the best fit regression to a value lower than 295.5 [32]. An alternative possibility is that some chlorine was left on or in sanidine crystals or adhered glass after the HCl treatment. During neutron bombardment, small amounts of ^{36}Ar are generated via β decay from ^{36}Cl produced by activation of ^{35}Cl [18]. Elevated ^{36}Ar in a few subsamples could have an effect similar to that of the hydration-induced fractionation described above. It is beyond the scope of this paper to attempt to resolve factors responsible for the low $^{40}Ar/^{36}Ar_i$ value defined by Spell and Harrison's [10] isochron. Because the experiments of [10] produced an isochron that raises several questions, but did not detect the presence of an excess argon component identified by our incremental-heating and laser fusion results, we conclude that the age of the Santa Rosa I dome is most reliably estimated at 936 ± 8 ka.

5.4. Implications for the geomagnetic reversal time scale

Renne et al. [26] recognized that the age reported by Spell et al. [9,10] for the Cerro Santa Rosa I dome did not date the end of the Jaramillo subchron, suggesting instead that it recorded the Kamikatsura Event [33]. On the basis of $^{40}Ar/^{39}Ar$ dates reported by Spell et al. [9,10], Izett and Obradovich [3] and the K–Ar and $^{40}Ar/^{39}Ar$ dates from four normally and transitionally magnetized lavas at Mt. Baker and Mt. Hood in the Cascade range [34], Singer et al. [6] proposed that the Santa Rosa I dome recorded a short period of transitional geomagnetic field behavior distinct from both the Jaramillo normal subchron and the Kamikatsura Event. The mean and standard deviation of the many age determinations [3,10, 34] were used to estimate the timing of this proposed Santa Rosa Event at about 936 ± 24 ka (adjusted to revised age for TCs standard). Despite the complication of excess argon in the Santa Rosa I rhyolite, our isochron age of 936 ± 8 ka not only confirms the earlier estimate, but reduces uncertainty concerning the timing of this event three-fold.

We are now able to distinguish at the 95% confidence level that the Santa Rosa Event post-dated termination of the Jaramillo normal subchron by 65 ± 13 kyr (Fig. 7). Moreover, given the range of ages for lavas that might record the Santa Rosa Event, particularly the youngest of these ages reported by [10], it remained uncertain how much time may have separated the Kamikatsura Event, at 899 ± 6 ka, from the Santa Rosa Event [6]. Our results demonstrate that at the 95% confidence level these two events recorded in transitionally magnetized lavas and separated in time from one another by a 910 ± 12 ka reversely magnetized lava on Haleakala volcano [6], took place 37 ± 9 kyr apart.

New high resolution paleointensity records of the geomagnetic field have been acquired from marine sediments around the globe. For example, sediments from the California margin [35], On-

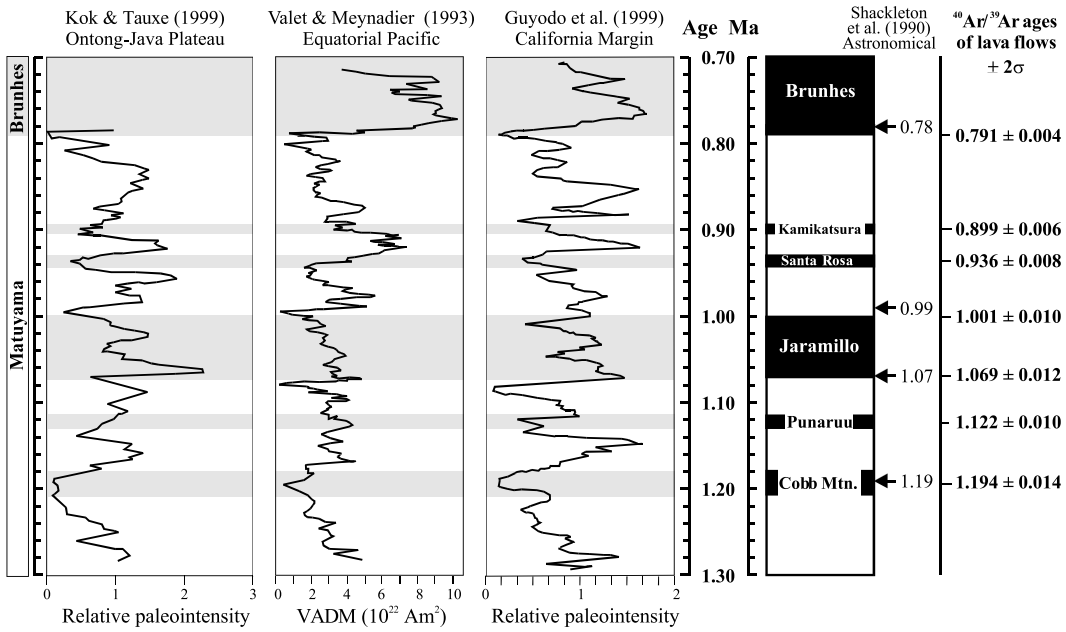

Fig. 7. Geomagnetic time scale for the upper Matuyama reversed chron. $^{40}Ar/^{39}Ar$ ages from terrestrial lavas are calculated relative to 28.34 Ma TCs [22] with $\pm 2\sigma$ analytical uncertainties, data from this study and Singer et al. [6]. Also shown are three paleointensity records from marine sediments [35–37] that have been scaled such that the intensity lows corresponding to the Matuyama-Brunhes reversal 791 ka and the Cobb Mountain Event 1.194 Ma match the time scale at the right. Prominent paleointensity lows coincide with the Kamikatsura, Santa Rosa, and other reversals or reversal attempts dated on land. Arrows denote astronomical ages [39] for polarity reversals at the Matuyama-Brunhes boundary, onset and termination of the Jaramillo normal subchron, and the Cobb Mountain Event.

tong-Java Plateau [36], and equatorial Pacific [37] all record a pair of prominent lows in relative paleointensity between the Jaramillo normal subchron and the Matuyama-Brunhes reversal (Fig. 7). Fixing the positions of the Matuyama-Brunhes reversal and Cobb Mountain normal subchron in the paleointensity records to a time scale consistent with our neutron fluence standard values, these two lows occur at about 890–900 ka and 930–940 ka, in accord with the geochronologic data presented here. In each record, a relative paleointensity high separates the two events (Fig. 7). We take these paleointensity records as strong evidence in support of our geochronologic and paleomagnetic results indicating that at least two short-lived paleomagnetic events characterized by transitional and relatively weak magnetic fields occurred about 40 kyr apart in the upper part of the Matuyama reversed chron.

One of the first terrestrial studies [38] in which $^{40}Ar/^{39}Ar$ dating corroborated the timing of the termination of the Jaramillo normal subchron and the Matuyama-Brunhes reversal predicted by the astronomical time scale of [39], also demonstrated that two short periods of nearly normal polarity occurred between ~980 ka and the Matuyama-Brunhes reversal (790 ka; recalculated for comparison to standard values used throughout this paper). Because these normal polarity events are recorded in lacustrine and fluvial sediments and tephra dates are limited [38], we can only speculate that one or both correspond to the Santa Rosa or Kamikatsura Events.

6. Conclusions

Paleomagnetic data acquired from seven sites on the the Cerro del Abrigo, Cerro Santa Rosa I and Cerro Santa Rosa II domes of the postcaldera collapse Valles rhyolite are consistent with the original results of Doell et al. [17]. Cerro

del Abrigo is normally magnetized, whereas the Santa Rosa I dome recorded a transitional magnetic field and the Santa Rosa II dome was erupted when the field was in a reversed polarity state.

$^{40}Ar/^{39}Ar$ laser fusion and incremental heating experiments on sanidine from the Cerro Santa Rosa I dome reveal that this rhyolite contained a small but significant component of excess argon prior to eruption. Despite the presence of excess argon in the sanidine crystals, using a recent intercalibration of neutron fluence standards, we determined the age of the Cerro Santa Rosa I dome to be 936 ± 8 ka (2σ). The latter age estimate is a factor of three more precise than the best previous value for the Santa Rosa Event, distinguishing it by 65 kyr from the preceding termination of the Jaramillo normal subchron 1001 ± 10 ka and by 37 kyr from younger basaltic lavas at Haleakala and Tahiti, which record the Kamikatsura Event 899 ± 6 ka. A pair of closely spaced lows in the paleointensity of marine sediments deposited between the Jaramillo normal subchron and Matuyama-Brunhes reversal most likely correspond to these events that are now temporally well defined on land. After four decades of investigation, re-investigation and serendipity, the Cerro Santa Rosa I rhyolite dome, once intimately linked with the end of the Jaramillo Event and the acceptance of plate tectonic theory, is now a highly resolved feature in its own right, and deserving as the namesake for the Santa Rosa Event.

Acknowledgements

We thank the Baca Land and Cattle Company for permission to sample on their property and Chris Condit, Cailey Condit, Ian Brown, and Jim Pickens for assistance in the field. Amy Fox Day-Lewis made all the paleomagnetic measurements. Brent Turrin generously supplied the ACs standard. Monica Relle completed the sanidine separation and with Brian Jicha and Mike Smith helped to measure neutron fluence monitors. Discussions with Paul Renne, Malcolm Pringle, and Ken Hoffman at various stages of this project were most helpful, as were reviews of the manuscript by Ajoy Baksi and John Geissman. We are grateful to Clark Johnson, John Valley, Lee Powell, Bill Unger, John Randall, and Monica Relle for their contributions in establishing the UW-Madison Rare Gas Geochronology Laboratory that was constructed with support from the NSF (grant EAR-9972851), UW-Madison Graduate School, the Lewis G. Weeks and Albert and Alice Weeks Foundations, Shell Oil Company, and Henry F. Nelson. Rock magnetic measurements were made at the Institute for Rock Magnetism, University of Minnesota, supported by the National Science Foundation and the Keck Foundation. This project was supported by NSF grants EAR-9805424 (L.L.B.) and EAR-9909309 (B.S.).*[SK]*

References

[1] R.R. Doell, G.B. Dalrymple, Geomagnetic polarity epochs: a new polarity event and the age of the Brunhes-Matuyama boundary, Science 152 (1966) 1060–1061.

[2] W. Glen, The Road to Jaramillo, Stanford University Press, Stanford, CA, 1982.

[3] G.A. Izett, J.D. Obradovich, $^{40}Ar/^{39}Ar$ age constraints for the Jaramillo Normal Subchron and the Matuyama-Brunhes geomagnetic boundary, J. Geophys. Res. 99 (1994) 2925–2934.

[4] C. Merrihue, G. Turner, Potassium–argon dating by activation with fast neutrons, J. Geophys. Res. 71 (1966) 2852–2857.

[5] A.K. Baksi, V. Hsu, M.O. McWilliams, E. Farrar, $^{40}Ar/^{39}Ar$ dating of the Brunhes-Matuyama geomagnetic field reversal, Science 256 (1992) 356–357.

[6] B.S. Singer, K.A. Hoffman, A. Chauvin, R.S. Coe, M.S. Pringle, Dating transitionally magnetized lavas of the late Matuyama Chron: toward a new $^{40}Ar/^{39}Ar$ timescale of reversals and events, J. Geophys. Res. 104 (1999) 679–693.

[7] S. Lund, G. Acton, B. Clement, M. Hastedt, M. Okada, T. Williams ODP Leg 172 Scientific Party,, Geomagnetic field excursions occurred often during the last million years, EOS Trans. Am. Geophys. Union 78 (1998) 178–179.

[8] D. Gubbins, The distinction between geomagnetic excursions and reversals, Geophys. J. Int. 137 (1999) F1–F3.

[9] T.L. Spell, I. McDougall, Revisions to the age of the Matuyama-Brunhes boundary and the Pleistocene polarity timescale, Geophys. Res. Lett. 19 (1992) 1181–1184.

[10] T.L. Spell, T.M. Harrison, $^{40}Ar/^{39}Ar$ geochronology of post-Valles caldera rhyolites, Jemez volcanic field, New Mexico, J. Geophys. Res. 98 (1993) 8031–8051.

[11] L. Tauxe, Paleomagnetic Principles and Practice, Kluwer Academic Publishers, Boston, MA, 1998.
[12] L. Tauxe, H. Staudigel, J.R. Wijbrans, Paleomagnetism and $^{40}Ar/^{39}Ar$ ages from La Palma in the Canary Islands, Geochem. Geophys. Geosyst. 1 (2000) paper No. 2000GC000063.
[13] R.A. Bailey, R.L. Smith, C.S. Ross, Stratigraphic Nomenclature of Volcanic Rocks in the Jemez Mountains, New Mexico, US Geol. Surv. Bull., 1274-P, 1969.
[14] R.L. Smith, R.A. Bailey, C.S. Ross, Geologic Map of the Jemez Mountains, New Mexico, US Geol. Surv. Misc. Invest. Map I-571, 1970.
[15] J.N. Gardner, F. Goff, S. Garcia, R.C. Hagan, Stratigraphic relations and lithologic variations in the Jemez Volcanic Field, New Mexico, J. Geophys. Res. 91 (1986) 1763–1778.
[16] G.F. Heiken, F. Goff, J.N. Gardner, W.S. Baldridge, J.B. Hulen, D.L. Nielson, D. Vaniman, The Valles/Toldeo Caldera Complex Jemez Volcanic Field, New Mexico, Ann. Rev. Earth Planet. Sci. 18 (1990) 27–53.
[17] R.R. Doell, G.B. Dalrymple, R.L. Smith, R.A. Bailey, Paleomagnetism, potassium–argon ages, and geology of rhyolites and associated rocks of the Valles Caldera, New Mexico, Mem. Geol. Soc. Am. 116 (1968) 211–248.
[18] I. McDougall, T.M. Harrison, Geochronology and Thermochronology by the $^{40}Ar/^{39}Ar$ Method, 2nd edn., Oxford University Press, Oxford, 1999.
[19] R.H. Steiger, E. Jäger, Subcommission on geochronology: convention on the use of decay constants in geo- and cosmochronology, Earth Planet. Sci. Lett. 36 (1977) 359–362.
[20] J.R. Taylor, An Introduction to Error Analysis, University Science Books, Mill Valley, CA, 1982.
[21] D. York, Least squares fitting of a straight line with correlated errors, Earth Planet. Sci. Lett. 5 (1969) 320–324.
[22] P.R. Renne, C.C. Swisher, A.L. Deino, D.B. Karner, T.L. Owens, D.J. DePaolo, Intercalibration of standards, absolute ages and uncertainties in $^{40}Ar/^{39}Ar$ dating, Chem. Geol. 145 (1998) 117–152.
[23] M.A. Lanphere, H. Baadsgaard, Precise K–Ar, $^{40}Ar/^{39}Ar$, Rb–Sr, and U–Pb mineral ages from the 27.5 Ma Fish Canyon Tuff reference standard, Chem. Geol. 175 (2001) 653–671.
[24] M.A. Lanphere, G.B. Dalrymple, First-principles calibration of ^{38}Ar tracers: implications for the ages of $^{40}Ar/^{39}Ar$ fluence monitors, US Geol. Surv. Prof. Paper 1621, 2000.
[25] A.K. Baksi, D.A. Archibald, E. Farrar, Intercalibration of $^{40}Ar/^{39}Ar$ dating standards, Chem. Geol. 129 (1996) 307–324.
[26] P.R. Renne, A.L. Deino, R.C. Walter, B.D. Turrin, C.C. Swisher, T.A. Becker, G.H. Curtiss, A.R. Jaouni, Intercalibration of astronomical and radioisotopic time, Geology 22 (1994) 783–786.
[27] J.A. Winick, W.C. McIntosh, N.W. Dunbar, Melt-inclusion: hosted excess ^{40}Ar in quartz crystals of the Bishop and Bandelier magma systems, Geology 29 (2001) 275–278.
[28] T.L. Spell, P.R. Kyle, M.F. Thirlwall, A.R. Campbell, Isotopic and geochemical constraints on the origin and evolution of postcollapse rhyolites in the Valles Caldera, New Mexico, J. Geophys. Res. 98 (1993) 19723–19739.
[29] I. Kaneoka, The effect of hydration on the K/Ar ages of volcanic rocks, Earth Planet. Sci. Lett. 14 (1972) 216–220.
[30] T.E. Cerling, F.H. Brown, J.R. Bowman, Low-temperature alteration of volcanic glass: hydration, Na, K, ^{18}O and Ar mobility, Chem. Geol. Isotop. Geosci. 52 (1985) 281–293.
[31] G. Turner, P.H. Cadogan, Possible effects of ^{39}Ar recoil in $^{40}Ar–^{39}Ar$ dating, Proc. 5th Lunar Sci. Conf. 2, 1974, pp. 1601–1615.
[32] P.E. Smith, D. York, Y. Chen, N.M. Evensen, R.C. Walter, $^{40}Ar/^{39}Ar$ dating of late Pleistocene volcanic glass from Santorini: a Theran hyalo-sphenochron, EOS Trans. Am. Geophys. Union 77 (1996) 794–795.
[33] D.E. Champion, M.A. Lanphere, M.A. Kuntz, Evidence for a new geomagnetic reversal from lava flows in Idaho: discussion of short polarity reversals in the Brunhes and late Matuyama polarity chrons, J. Geophys. Res. 93 (1988) 11667–11680.
[34] M.A. Lanphere, D.E. Champion, W. Hildreth, New evidence on the magentic reversal time scale from volcanic rocks in the Cascade range, Washington, Oregon, and California, EOS Trans. Am. Geophys. Union 78 (1997) 196.
[35] Y. Guyodo, C. Richter, J.P. Valet, Paleointensity record from Pleistocene sediments (1.4–0 Ma) of the California Margin, J. Geophys. Res. 104 (1999) 22953–22964.
[36] Y.S. Kok, L. Tauxe, A relative paleointensity stack from Ontong-Java Plateau sediments for the Matuyama, J. Geophys. Res. 104 (1999) 25401–25413.
[37] J.P. Valet, L. Meynadier, Geomagnetic field intensity and reversals during the past four million years, Nature 366 (1993) 234–238.
[38] L. Tauxe, A.D. Deino, A.K. Beherensmeyer, R. Potts, Pinning down the Brunhes/Matuyama and upper Jaramillo boundaries: a reconciliation of orbital and isotopic time scales, Earth Planet. Sci. Lett. 109 (1992) 561–572.
[39] N.J. Shackleton, A. Berger, W.R. Peltier, An alternative astronomical calibration of the lower Pleistocene timescale based on ODP site 677, Trans. R. Soc. Edinburgh Earth Sci. 81 (1990) 251–261.
[40] R. Day, M.D. Fuller, V.A. Schmidt, Hysteresis properties of titanomagnetites: grain size and composition dependence, Phys. Earth Planet. Int. 13 (1977) 260–267.
[41] R.A. Fisher, Dispersion on a sphere, Proc. R. Soc. Lond. A217 (1953) 295–305.